Revealing the electronic properties of the B-B bond:

the bis-catecholato diboron molecule

D. Toffoli[1], C. Grazioli[2], M. Monti[1], M. Stener[1], R. Totani[3], R.Richter[4], L. Schio[2], G. Fronzoni[1,a)], A. Cossaro[1,2,a)]

AFFILIATIONS

[1] *Department of Chemical and Pharmaceutical Sciences, University of Trieste, 34127 Trieste, Italy*
[2] *IOM-CNR, Istituto Officina dei Materiali-CNR, S.S.14, Km 163.5, 34149 Trieste, Italy*
[3] *ISM-CNR, Istituto di Struttura della Materia, LD2 Unit, 34149 Trieste, Italy*
[4] *Elettra-Sincrotrone Trieste, 34149 Basovizza, Trieste, Italy*

a) Authors to whom correspondence should be addressed: fronzoni@units.it; acosssaro@units.it

Electronic Supplementary Information
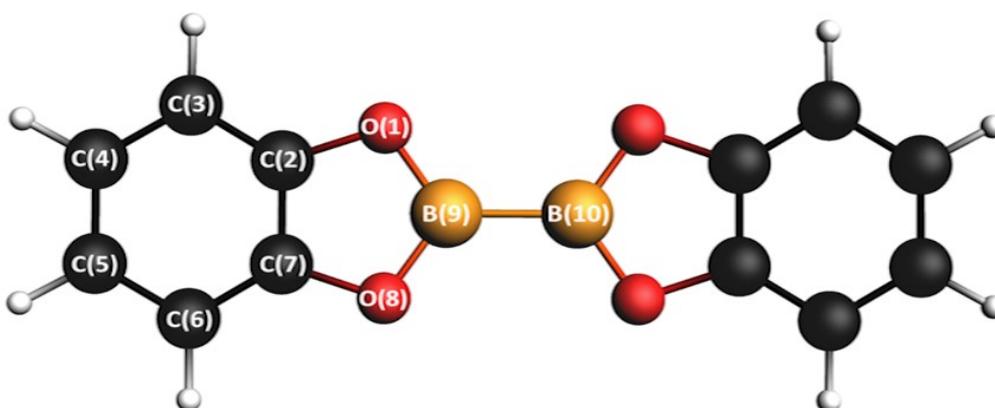
1. Geometry optimization of B_2Cat_2

Figure S1. *Chemical structure of B_2Cat_2. Labels on the atoms refer to geometrical parameters listed in Table S1.*

Table S1. *Comparison between theoretical and experimental geometrical parameters for B2Cat2. Bond lengths are expressed in Å and bond angles in degrees (°).*

Bond lengths[a]	Calculated	Experimental[b]
B(9)-B(10)	1.685	1.678
O(8)-C(7)	1.382	1.387
O(1)-C(2)	1.382	1.386
C(7)-C(6)	1.381	1.372
C(6)-C(5)	1.398	1.391
C(5)-C(4)	1.398	1.393
C(4)-C(3)	1.398	1.393
C(3)-C(2)	1.381	1.376
C(2)-C(7)	1.390	1.384
O(8)-B(9)	1.391	1.382
O(1)-B(9)	1.390	1.394
Bond angles[a]	Calculated	Experimental[b]
B(10)-B(9)-O(8)	124.5	124.6
B(10)-B(9)-O(1)	124.5	124.2
B(9)-O(8)-C(7)	105.5	105.5
B(9)-O(1)-C(2)	105.5	105.1
O(8)-B(9)-O(1)	111.0	111.2
O(8)-C(7)-C(6)	128.9	128.7
O(1)-C(2)-C(3)	128.9	128.6
O(8)-C(7)-C(2)	109.0	108.9
O(1)-C(2)-C(7)	109.0	109.2
C(7)-C(2)-C(3)	122.1	122.1
C(2)-C(7)-C(6)	122.1	122.4

C(7)-C(6)-C(5)	116.5	116.2
C(6)-C(5)-C(4)	121.4	121.6
C(5)-C(4)-C(3)	121.4	121.5
C(4)-C(3)-C(2)	116.5	116.2

[a] Labels of the atoms refer to those reported in Figure S1.
[b] W. Clegg et Al. *Inorg. Chem*. **1994**, *33*, 4623-4624.

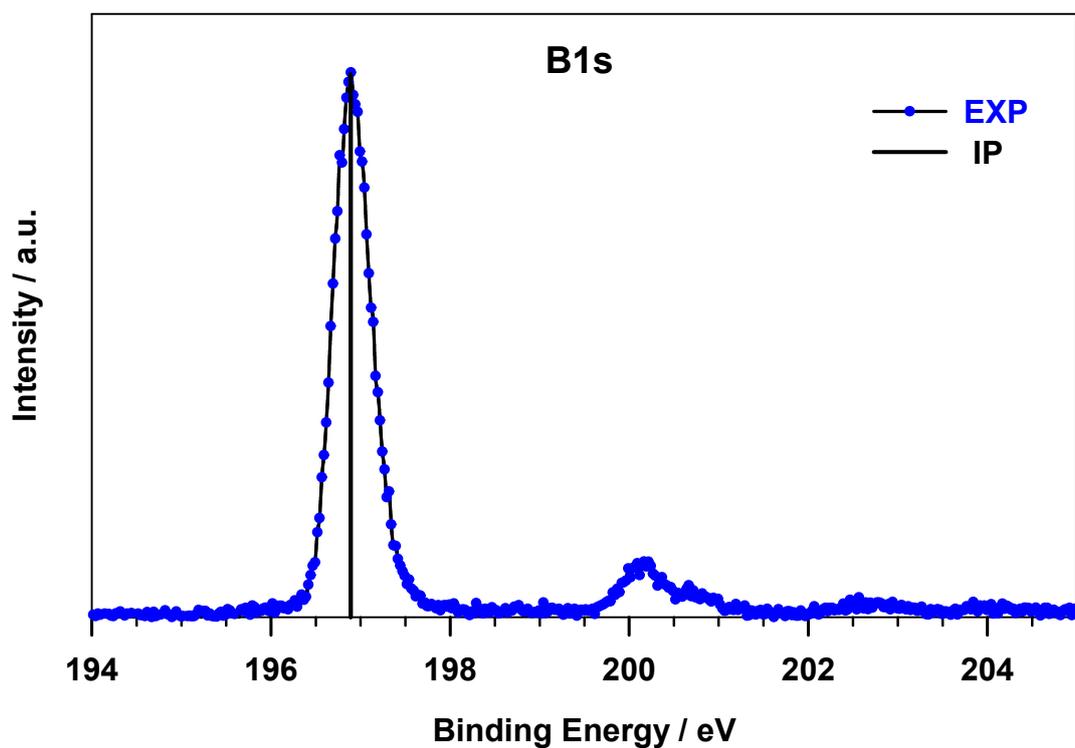## 2. Experimental and theoretical XPS Spectra

Figure S2. B1s photoelectron spectrum of B_2Cat_2. Vertical black line: B1s calculated ΔSCF IP (196.52 eV) shifted by +0.37 eV in order to match the experimental peak.
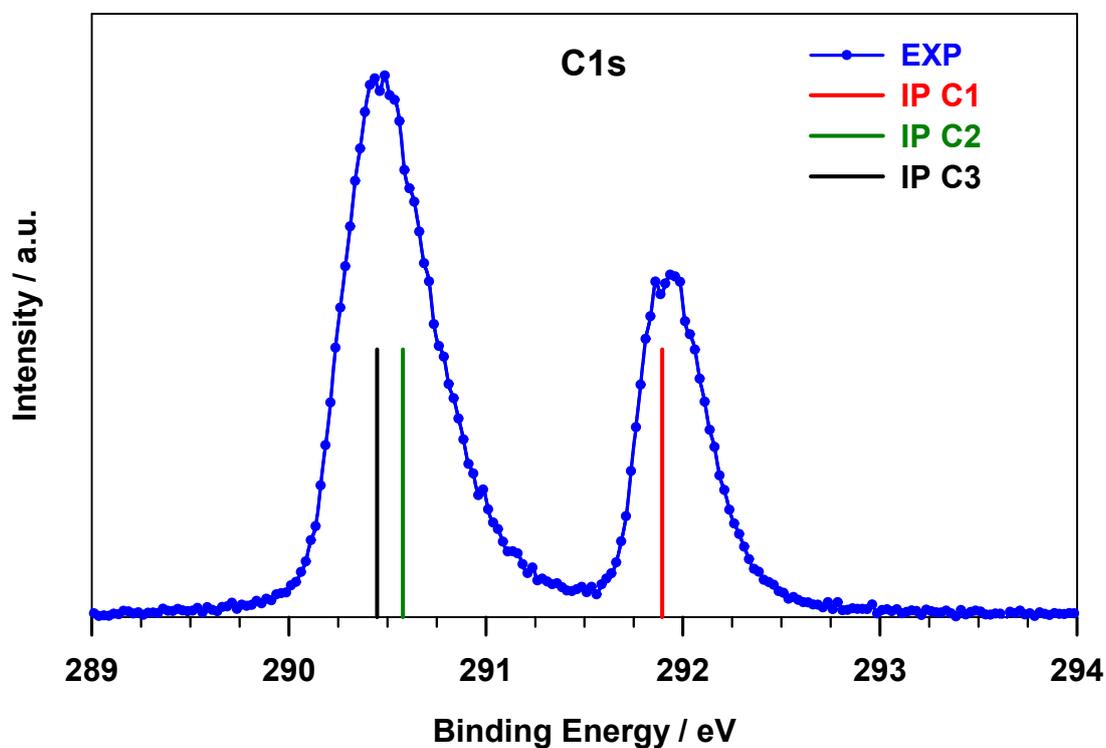

Figure S3. C1s photoelectron spectrum of B_2Cat_2. Vertical colored lines:C1s calculated ΔSCF IPs (C1 : 291.89 eV; C2: 290.58 eV; C3: 290.45 eV)
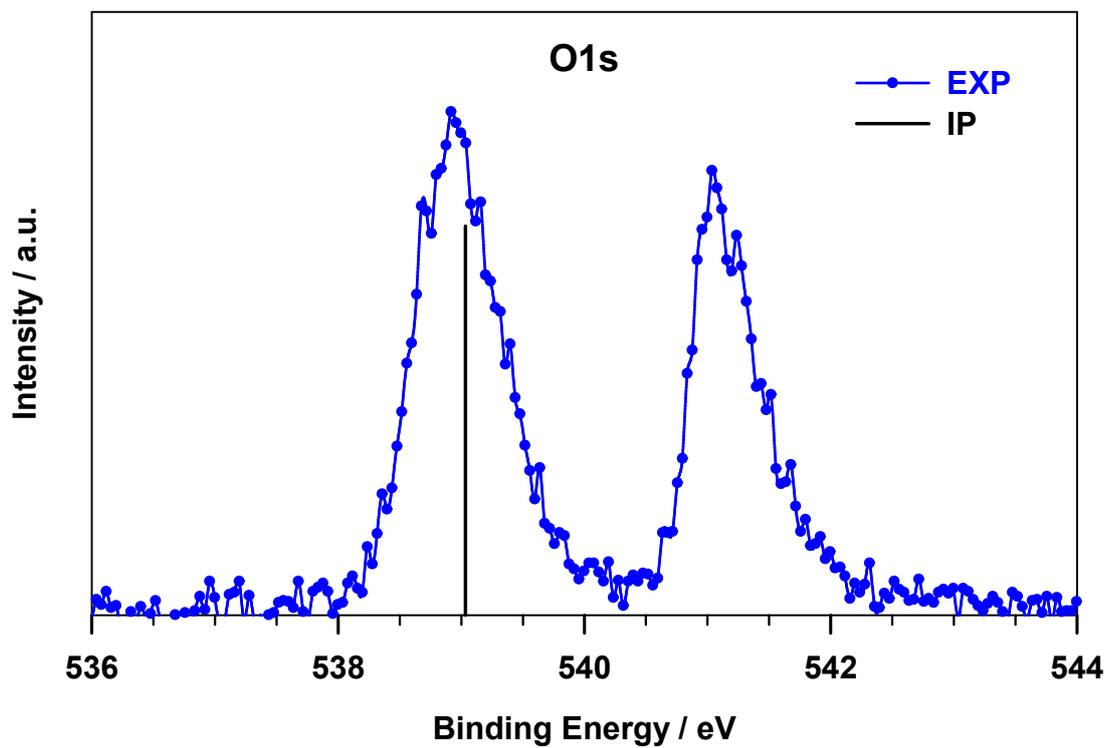
Figure S4. O1s photoelectron spectrum of B_2Cat_2. Vertical black line: O1s calculated ΔSCF IP (539.03 eV).

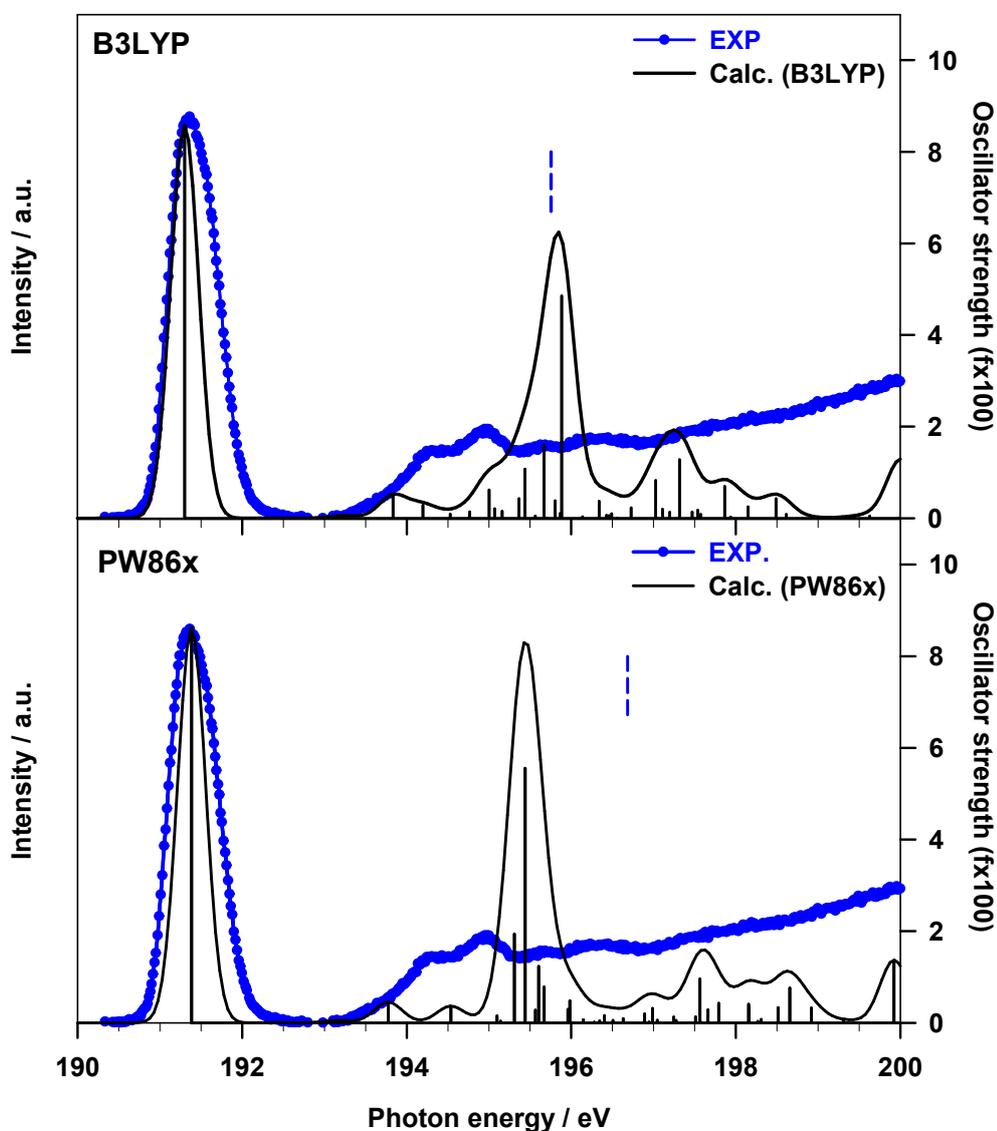## 3. DFT-TP B K-Edge NEXAFS spectrum with different xc functionals

Figure S5. DFT-TP NEXAFS B1s spectra of B_2Cat_2. Upper panel: B3LYP; lower panel PW86. The experimental spectrum is reported for comparison The calculated spectra were rigidly shifted on the experimental energy scale (B3LYP: 0.76 eV; PW86 +0.17 eV). Vertical blue lines: IP experimental values. The stick spectra are broadened by using a Gaussian lineshape with FWHM=0.4 eV.

4. Details on the TDDFT calculations and Results

The B1s core excitations of B_2Cat_2 have also been calculated by employing the Time-Dependent DFT (TDDFT) method, which formally includes the coupling between single excited configurations. The core excited states can be efficiently computed by reducing the 1h-1p space to include only the configurations generated by the excitations from the subset of core orbitals[1]. In this way the coupling between core excitations and valence excitations to the continuum is neglected and the computational scheme does not need the treatment of the continuum states. The TDDFT scheme employed for the calculations of the B K-edge spectrum consists of the excitations from both the core orbitals of the two B atoms (coupled scheme).

In the TDDFT calculations, the adiabatic local density approximation (ALDA) to the exchange-correlation (xc) kernel has been employed[2]. For the xc potential applied in the self-consistent field (SCF) calculations, three different xc functionals with the ground state electron configuration have been considered: the LB94[3], chosen for its correct asymptotic behaviour, the hybrid B3LYP, and the range-separated hybrid CAM-B3LYP xc functionals. The TDDFT calculations have been performed by using a TZP basis set for all atoms.

The calculated B1s NEXAFS spectra are collected in Figure S6 and compared with the gas-phase experiment. The influence of the different xc functionals is also tested. The inspection of the figure reveals that the disagreement between theory and experiment persists also at TDDFT level, irrespective of the xc functional employed, in particular the incorrect intensity distribution between the first two peaks as well as the overestimate of their energy separation. Bearing in mind the DFT-TP results, no improvement is therefore obtained at the TDDFT level, suggesting that the configuration mixing introduced at the TDDFT level (within the ALDA approximation) is not adequate to properly describe the B1s core excitations, as already found in previous calculations on boronic-acid derivatives[4] . It is interesting to observe that the nature of the excitations at the TDDFT level is consistent with that obtained at the DFT-TP level, confirming the assignment of the experimental spectrum.
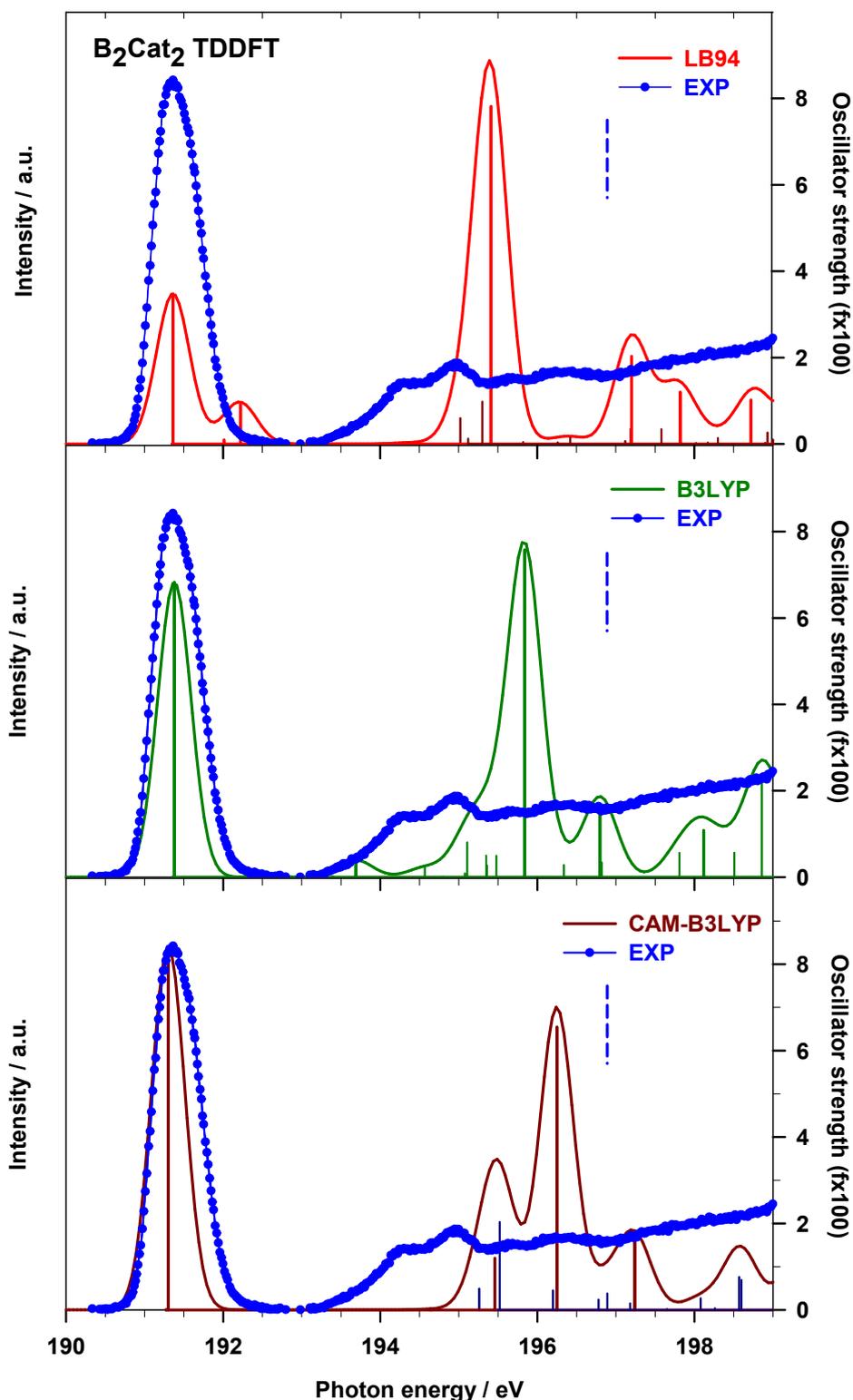
Figure S6. B1s NEXAFS spectra of B_2Cat_2 calculated at the TDDFT level by employing different xc potentials. The experimental spectrum is reported for comparison. A rigid shift has been applied to the calculated B1s profiles to align the energy position of the first absorption peak to the experimental one (2.44 eV for LB94; 9.81 eV for B3LYP; 9.64 eV for CAM-B3LYP). Vertical blue lines: IP (B1s) experimental value. The stick spectra are broadened by using a Gaussian lineshape with FWHM=0.5 eV.
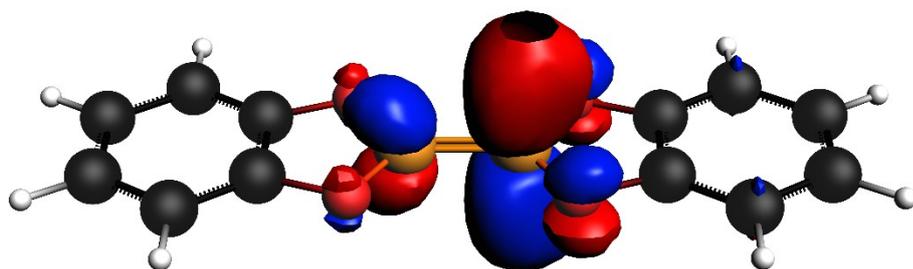
5. 3D plots of selected final MOs corresponding to the B1s, C1s and O1s core excitation calculations
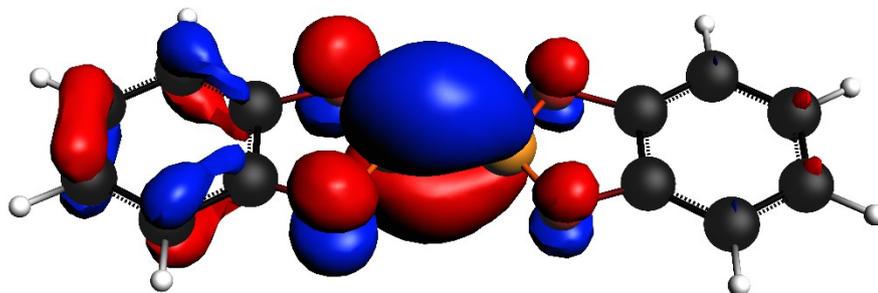
7 b1 (ΔSCF transition at 191.33 eV)
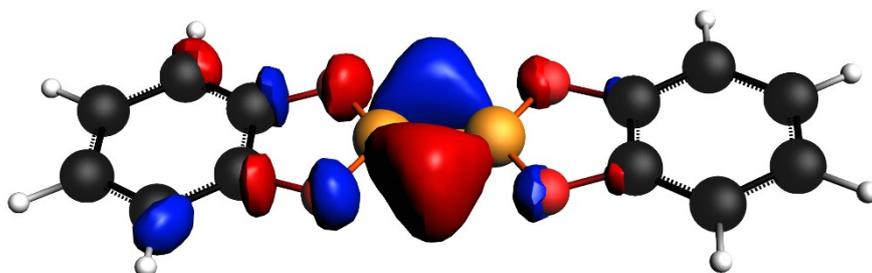
23 b_2 (ΔSCF transition at 194.78 eV)

11 b_1 (ΔSCF transition at 195.31 eV)

Figure S7. 3D plots of final MOs (with a core-hole on the B site of B_2Cat_2) obtained from the ΔSCF calculations . Displayed isosurface corresponds to ±0.030 $e^{1/2}a_0^{-3/2}$ value.
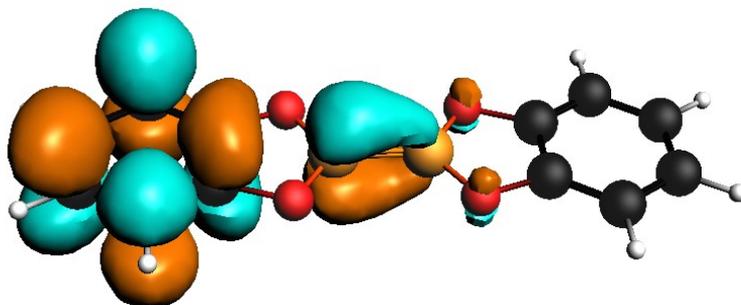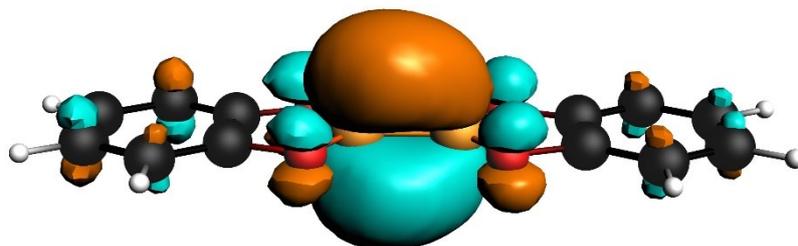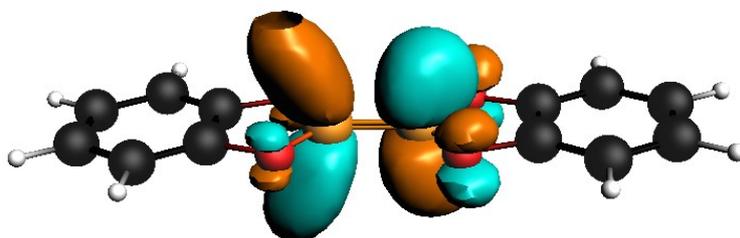
Figure S8. 3D plot of the LUMO MO of B_2Cat_2 (with a core-hole on C2) from the DFT-TP calculations. Displayed isosurface corresponds to ±0.030 $e^{1/2}a_0^{-3/2}$ value.

LUMO (transition at 534.34 eV)

LUMO + 17 (transition at 538.60 eV)

Figure S9. 3D plots of LUMO and LUMO+17 MOs of B_2Cat_2 (with a core-hole on the O site) from the DFT-TP calculations. Displayed isosurface corresponds to ±0.030 $e^{1/2}a_0^{-3/2}$ value.

6. Experimental details

The BCDB molecule, in the form of a powder, was purchased from TCI, purity >98%, and sublimated in vacuum by means of a Knudsen cell heated at 330 K. The molecule was studied in the isolated form at the Gas Phase beamline[5] at Elettra. The sublimation rate was optimized checking the mass spectrum by means of a home-made time-of-flight spectrometer (TOF). The powder was purified for one night and the spectra collection started after no trace of contamination in the photoemission signal was detected. The high-resolution N 1s, C 1s, and B 1s XPS and valence band spectra were recorded with a VG-220i hemispherical electron energy analyzer mounted in the plane perpendicular to the photon propagation direction at the magic angle (i.e. 54.7° with respect to the electric vector

of the light). In this geometry, photoemission measurements are insensitive to the photoelectron asymmetry β parameter. NEXAFS spectra at the N, C and B *K* edges were collected using the same TOF described before in a total-ion-yield configuration. The photon energies and resolutions used for the core excitation spectra are reported in Table S2. More details about the end station are available in Ref.[6]

Table S2. *Gas phase experimental parameters*

PES				
Spectral region	Photon en. [eV]	Overall resolution [meV]	Calibrant	Binding en. [eV]
B1s	262	130	SF6 (2p3/2)	180.21 eV [7,8]
C1s	390	150	CO2 (C1s)	297.7 eV[9]
O1s	628	240	CO2 (O1s)	541.08 eV [7]
VB	97	100	N2 (p_{BOND})	15.60 [10]
VB (ResPES)	189.3 191.3	360		
NEXAFS				
B K	190-210	20	SF6 ($2p_{1/2} \rightarrow t_{2g}$)	184.57[11]
C K	283-300	50	CO2 (C1s$\rightarrow\pi$)	290.77 [12]
O K	532-540	90	CO2 (O 1s$\rightarrow\pi_u$)	535.4 [13]

The presented data refer to the saturation coverage of a monolayer. B_2Cat_2 was deposited on clean Au(111) single crystal surface by sublimation from a Knudsen cell heated at 330 K, with the substrate kept at room temperature. In these conditions, molecules beyond the first layer do not stick, that was confirmed spectroscopically by monitoring the intensity of the XPS peaks. Measurements were performed at the ANCHOR-SUNDYN endstation[14] of the ALOISA beamline at Elettra Synchrotron. XPS measurements were performed at photon energies of 650 eV for O1s and at 400 eV for C1s and B1s, with an overall resolution of 0.2 and 0.15 eV respectively. NEXAFS spectra were acquired in Auger yield, with photon resolution of 0.15 and 0.1 eV for O K-edge and B (C) K-edge respectively. In order to investigate dichroic effects the NEXAFS spectra were acquired at two different geometries: with the sample surface oriented either parallel to the light electric field plane (s-polarization) or closely normal to it (p-polarization).

References

1   M. Stener, G. Fronzoni and M. de Simone, Time dependent density functional theory of core electrons excitations, *Chem. Phys. Lett.*, 2003, **373**, 115–123.

2   E. K. U. Gross and W. Kohn, in *Density Functional Theory of Many-Fermion Systems*, ed. P.-O. Löwdin, Academic Press, 1990, vol. 21, pp. 255–291.

3   R. van Leeuwen and E. J. Baerends, Exchange-correlation potential with correct asymptotic behavior, *Phys. Rev. A*, 1994, **49**, 2421–2431.

4   D. Toffoli, A. Ponzi, E. Bernes, M. De Simone, C. Grazioli, M. Coreno, M. Stredansky, A. Cossaro and G. Fronzoni, Correlation effects in B1s core-excited states of boronic-acid derivatives: An experimental and computational study, *J. Chem. Phys.*, , DOI:10.1063/1.5120175.

5   K. C. Prince, R. R. Blyth, R. Delaunay, M. Zitnik, J. Krempasky, J. Slezak, R. Camilloni, L. Avaldi, M. Coreno, G. Stefani, C. Furlani, M. De Simone and S. Stranges, The gas-phase photoemission beamline at Elettra., *J. Synchrotron Radiat.*, 1998, **5**, 565–8.

6   O. Plekan, H. Sa'adeh, A. Ciavardini, C. Callegari, G. Cautero, C. Dri, M. Di Fraia, K. C. Prince, R. Richter, R. Sergo, L. Stebel, M. Devetta, D. Faccialà, C. Vozzi, L. Avaldi, P. Bolognesi, M. C. Castrovilli, D. Catone, M. Coreno, F. Zuccaro, E. Bernes, G. Fronzoni, D. Toffoli and A. Ponzi, Experimental and Theoretical Photoemission Study of Indole and Its Derivatives in the Gas Phase, *J. Phys. Chem. A*, 2020, **124**, 4115–4127.

7   L. Pettersson, J. Nordgren, L. Selander, C. Nordling, K. Siegbahn and H. Ågren, Core-electron binding energies in the soft X-ray range obtained in X-ray emission, *J. Electron Spectros. Relat. Phenomena*, , DOI:10.1016/0368-2048(82)85050-0.

8   J. E. True, T. D. Thomas, R. W. Winter and G. L. Gard, Electronegativities from core-ionization energies: Electronegativities of SF5 and CF3, *Inorg. Chem.*, , DOI:10.1021/ic0343298.

9   V. Myrseth, J. . Bozek, E. Kukk, L. . Sæthre and T. . Thomas, Adiabatic and vertical carbon 1s ionization energies in representative small molecules, *J. Electron*

Spectros. Relat. Phenomena, 2002, **122**, 57–63.

10   H.-H. Perkampus, D. W. Turner: Molecular Photoelectron Spectroscopy. Unter Mitarbeit von C. Baker, A. D. Becker und C. R. Brundle, Wiley-Interscience, John Wiley & Sons Ltd., London, New York, Sydney, Toronto 1970. 386 Seiten. Preis: 140 sh., *Berichte der Bunsengesellschaft für Phys. Chemie*, 1971, **75**, 181– 181.

11   E. Hudson, D. A. Shirley, M. Domke, G. Remmers, A. Puschmann, T. Mandel, C. Xue and G. Kaindl, High-resolution measurements of near-edge resonances in the core-level photoionization spectra of SF6, *Phys. Rev. A*, 1993, **47**, 361–373.

12   M. Tronc, G. C. King and F. H. Read, Carbon K-shell excitation in small molecules by high-resolution electron impact, *J. Phys. B At. Mol. Phys.*, 1979, **12**, 137–157.

13   G. R. Wight and C. E. Brion, K-Shell energy loss spectra of 2.5 keV electrons in CO2 and N2O, *J. Electron Spectros. Relat. Phenomena*, 1974, **3**, 191–205.

14   R. Costantini, M. Stredansky, D. Cvetko, G. Kladnik, A. Verdini, P. Sigalotti, F. Cilento, F. Salvador, A. De Luisa, D. Benedetti, L. Floreano, A. Morgante, A. Cossaro and M. Dell'Angela, ANCHOR-SUNDYN: A novel endstation for time resolved spectroscopy at the ALOISA beamline, *J. Electron Spectros. Relat. Phenomena*, 2018, **229**, 7–12.